International Journal of Mathematical Archive-6(5), 2015, 87-101
Available online through www.ijma.info ISSN 2229 – 5046

MODIFIED REYNOLDS EQUATION FOR SQUEEZE FILM LUBRICATION BETWEEN DOUBLE LAYERED POROUS RECTANGULAR PLATES WITH COMBINED EFFECT OF MHD AND CCSF

SYEDA TASNEEM FATHIMA*[1], N. B NADUVINAMANI[2], H. M. SHIVAKUMAR[3], B. N. HANUMAGOWDA[4]

[1]Department of Mathematics,
Reva Institute of Technology and Management, Bangalore-560064, India.

[2]Department of Mathematics,
Gulbarga University, Gulbarga-585106, India.

[3]Department of Mathematics,
East West Institute of Technology, Bangalore -560091, India.

[4]Department of Mathematics,
East Point College of Engineering & Technology, Bangalore - 560049, India.

(Received On: 20-04-15; Revised & Accepted On: 21-05-15)

ABSTRACT

The squeeze film characteristics of double layer porous rectangular plates with combined effect of conducting couplestress fluid (CCSF) and transverse magnetic field are theoretically investigated .The Modified MHD Reynolds type equation is derived and closed form solution for the squeeze film pressure, load carrying capacity and squeeze film time are obtained. From the results obtained, it is observed that, there is significant increase in the squeeze film characteristics for increasing values of couplestress parameter as compared to non-conducting lubricant (NCL) case in the presence of transverse magnetic field. Whereas the effect of permeability parameter is to decrease these squeeze film characteristics.

Key Words: *Double layered porous; rectangular plates; couplestress; and magnetic parameter.*

1. INTRODUCTION

Squeeze film characteristics play an important role in many applications, such as lubrication of machine elements, automatic transmissions, and artificial joints. A positive pressure can be generated in a fluid contained between two surfaces when the surfaces are moving towards each other. A finite time is required to squeeze the fluid out of the gap, and this action provides a useful cushioning effect in the bearings. The reverse effect, which occurs when the surfaces are moving apart, can lead to cavitations in liquid films. For squeeze film bearings a relationship needs to be developed between load and normal velocity at any instant. The squeeze film phenomenon has applications in all reciprocating machines.

Corresponding Author: Syeda Tasneem Fathima[1], [1]Department of Mathematics,
Reva Institute of Technology and Management, Bangalore-560064, India.*

Porous bearings have been widely used in industry for a long time. Porous bearings contain the porous medium filled with lubricating oil so that the bearing requires no further lubrication during the whole life of the machine. Self lubricated bearings or oil retaining bearings exhibit this feature. Sintered metal self lubricating bearings are advantageous for many applications such as vacuum cleaners, extractor fans, motor car starters, hair dryers and business machines, owing to the low initial cost, simplicity and ease of lubrication. Also self lubricating porous bearings have the advantage of high production rate because, short sintering time is required. Graphite is added to enhance the self lubricating property of the bearings. The lubricant penetrates into the pores and remains effective throughout the bearing life. Graphite is added to enhance the self lubricating property of the bearings. The analytical study of porous bearings with hydrodynamic conditions was first made by Morgan and Cameron[1].

An extensive study of porous bearing has been made during the last few decades [2-5]. The lubricant penetrates in to the pores and remains effective throughout the bearing life. Although the bearing characteristics suffer because of porosity, the numerous design and maintenance advantages over come these. Cusano[6] has shown that the seepage through the boundary of the porous bearing may be decreased by the use of porous housings of different permeabilities to improve bearing performance.

Couplestress fluids are a consequence of the assumption that the interaction of one part of the body on another, across a surface is equivalent to a force and momentum distribution. Couple stresses may appear particularly in problems where thin film exists. Many authors have used this couple stress model to study the various hydrodynamic lubrication problems[7-10]. Efforts have been made to improve bearing characteristics by application of electromagnetic fields[11-14]; Sinha and Guptha[15] have shown that the load capacity and time of approach can be increased by the use of MHD.

Owing to the development of modern machine elements, different types of lubricants are selected to meet the specific requirements for bearing operating under various severe conditions. To avoid unexpected viscosity variation with temperature, the use of liquid metals as lubricants has received extensive interest. Compared with the conventional non-conducting lubricating oils, liquid metals possess a higher thermal conductivity and a higher electrical conductivity. The property of high thermal conductivity reveals that the heat from the source of generation is readily conducted away. In addition, the property of high electrical conductivity implies that hydrodynamic flow behaviour can be adjusted by the application of an external magnetic field. Since the motion of an electrically conducting liquid across a magnetic field will evoke an electrical-field intensity. This electrical field intensity results in a current density interacting with the magnetic field to produce a Lorentz body force. By properly orienting the applied magnetic field, this Lorentz body force acting on the lubricant film may provide a component opposite to the direction of motion. As a consequence, the hydrodynamic characteristics of thin film bearings with electrically conducting lubricants can be improved by the application of thin film bearings with electrically conducting lubricants by the application of external magnetic fields. Recently, Naduvinamani *et al.*[16] studied the effect of Magneto-hydrodynamic couple stress on squeeze film lubrication of bearings in circular stepped plates and found that combined effect of couplestress and MHD is to increase the load carrying capacity and squeeze film time.

Hence, the aim of this paper is to obtain the Modified Reynolds Equation for the squeeze film lubrication between double-layered porous rectangular plates with the combined effect of MHD and CCSF, when the upper plate has a porous housing of two layers with different permeabilities. Using the Stokes couplestress fluid model and MHD flow model, it is shown that the combined effect of CCSF and applied magnetic field enhances the load carrying capacity and time of approach in case of double layered porous plates. In order to highlight the significance of conducting couple stresses and transverse magnetic field, the results are compared with conventional Newtonian non-conducting lubricant (NCL).

2. FORMULATION OF THE PROBLEM

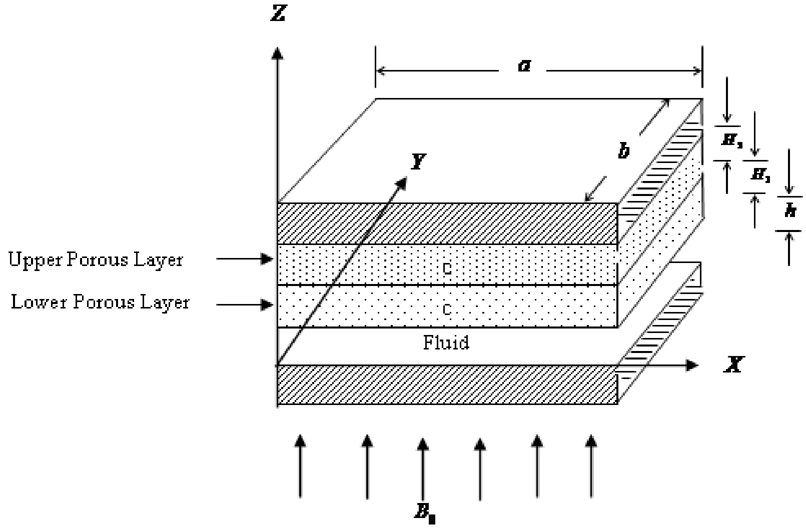

Fig.1. Physical configuration of double layered porous plates

Consider a fluid film of thickness h between two rectangular plates, where the lower plate remains fixed and the upper plate is assumed to move normal to itself. The upper plate has a double–layer porous housing with permeabilities k_1 and k_2 of the lower and upper layers respectively. A uniform magnetic field B_0 is applied perpendicular to the plates. The physical configuration of squeeze film lubrication between to plates with double layer porous region with MHD is shown in Figure.1. Flow in the porous regions follows the modified Darcy's law. In the film region the equations of hydromagnetic lubrication theory hold. Following the assumptions MHD and Stokes couplestress theory, the basic equations governing the hydromagnetic flow of the conducting couplestress lubricant in different regions are:
Film region,

$$\mu\frac{\partial^2 u}{\partial z^2}-\eta\frac{\partial^4 u}{\partial z^4}-\sigma B_0^2 u=\frac{\partial p}{\partial x} \tag{1}$$

$$\mu\frac{\partial^2 v}{\partial z^2}-\eta\frac{\partial^4 v}{\partial z^4}-\sigma B_0^2 u=\frac{\partial p}{\partial y} \tag{2}$$

$$\frac{\partial p}{\partial z}=0 \tag{3}$$

$$\frac{\partial u}{\partial x}+\frac{\partial v}{\partial y}+\frac{\partial w}{\partial z}=0 \tag{4}$$

Boundary Conditions are:

i) At the upper surface $Z=h$

$$u=v=0 \qquad \frac{\partial^2 u}{\partial z^2}=\frac{\partial^2 v}{\partial z^2}=0 \tag{4a}$$

ii) At the lower surface $Z=0$

$$u=v=0 \qquad \frac{\partial^2 u}{\partial z^2}=\frac{\partial^2 v}{\partial z^2}=0 \tag{4b}$$

Lower porous region:

$$u_1=\frac{-k_1}{\mu\left(1-\beta+\dfrac{k_1 M_0^2}{m_1 h_0^2}\right)}\frac{\partial P_1}{\partial x} \tag{5}$$

$$v_1=\frac{-k_1}{\mu\left(1-\beta+\dfrac{k_1 M_0^2}{m_1 h_0^2}\right)}\frac{\partial P_1}{\partial y} \tag{6}$$

$$w_1 = \frac{-k_1}{\mu(1-\beta)}\frac{\partial P_1}{\partial z} \tag{7}$$

$$\frac{\partial u_1}{\partial x}+\frac{\partial v_1}{\partial y}+\frac{\partial w_1}{\partial z}=0 \tag{8}$$

Upper porous region:

$$u_2 = \frac{-k_2}{\mu\left(1-\beta+\dfrac{k_2 M_0^2}{m_2 h_0^2}\right)}\frac{\partial P_2}{\partial x} \tag{9}$$

$$v_2 = \frac{-k_2}{\mu\left(1-\beta+\dfrac{k_2 M_0^2}{m_2 h_0^2}\right)}\frac{\partial P_2}{\partial y} \tag{10}$$

$$w_2 = \frac{-k_2}{\mu(1-\beta)}\frac{\partial P_2}{\partial z} \tag{11}$$

$$\frac{\partial u_2}{\partial x}+\frac{\partial v_2}{\partial y}+\frac{\partial w_2}{\partial z}=0 \tag{12}$$

3. SOLUTION

The solution of equations (1) and (2) subject to the no-slip condition (4a) and (4b) on both the surface is obtained as

$$u = -\frac{h_0^2}{\mu M_0^2}\frac{\partial p}{\partial x}\left\{\frac{1}{(A^2-B^2)}\left(\frac{B^2 Cosh\dfrac{A(2z-h)}{2l}}{Cosh\dfrac{Ah}{2l}}-\frac{A^2 Cosh\dfrac{B(2z-h)}{2l}}{Cosh\dfrac{Bh}{2l}}\right)+1\right\} \tag{13}$$

and

$$v = -\frac{h_0^2}{\mu M_0^2}\frac{\partial p}{\partial y}\left\{\frac{1}{(A^2-B^2)}\left(\frac{B^2 Cosh\dfrac{A(2z-h)}{2l}}{Cosh\dfrac{Ah}{2l}}-\frac{A^2 Cosh\dfrac{B(2z-h)}{2l}}{Cosh\dfrac{Bh}{2l}}\right)+1\right\} \tag{14}$$

Substituting equations (13) and (14) into equation (4) and integrating across the film thickness h (remembering that the lower plate is non-porous and fixed), we obtain

$$w_h - w_0 = \frac{h_0^2}{\mu M_0^2}\left(\frac{\partial^2 p}{\partial x^2}+\frac{\partial^2 p}{\partial y^2}\right) f(h,l,M_0) \tag{15}$$

where

$$f(h,l,M_0) = \frac{2l}{(A^2-B^2)}\left(\frac{B^2}{A}\tanh\frac{Ah}{2l}-\frac{A^2}{B}\tanh\frac{Bh}{2l}\right)+h$$

Since the velocity component in the z- direction is continuous at the plate-film interface,

$$w\big|_{z=h} - \frac{dh}{dt} = w_1\big|_{z=h} = -\frac{k_1}{\mu}\left(\frac{\partial P_1}{\partial z}\right)_{z=h} \tag{16}$$

From equations (15) and (16), the fluid pressure in the film region is found to satisfy the equation

$$\frac{\partial^2 p}{\partial x^2}+\frac{\partial^2 p}{\partial y^2} = \frac{\dfrac{dh}{dt}-\dfrac{k_1}{\mu}\left(\dfrac{\partial P_1}{\partial z}\right)_{z=h}}{\dfrac{h_0^2}{\mu M_0^2}f(h,l,M_0)} \tag{17}$$

Equation (17) is the required Modified Reynolds Equation for combined effect of CCSF and MHD.

From equations (5) - (12) it follows that the fluid pressure in the porous regions satisfy the equations

$$\frac{\partial^2 P_1}{\partial x^2}+\frac{\partial^2 P_1}{\partial y^2}+C_1^2\frac{\partial^2 P_1}{\partial z^2}=0 \tag{18}$$

and

$$\frac{\partial^2 P_2}{\partial x^2}+\frac{\partial^2 P_2}{\partial y^2}+C_2^2\frac{\partial^2 P_2}{\partial z^2}=0 \tag{19}$$

Where

$$C_1=\left(\frac{1-\beta+\frac{k_1 M_0^2}{m_1 h_0^2}}{1-\beta}\right)^{1/2} \tag{20}$$

and

$$C_2=\left(\frac{1-\beta+\frac{k_2 M_0^2}{m_2 h_0^2}}{1-\beta}\right)^{1/2} \tag{21}$$

The boundary conditions associated with Equations. (17) - (19) are

$$p(x,0)=0 \tag{22}$$
$$p(x,b)=0 \tag{23}$$
$$p(0,y)=0 \tag{24}$$
$$p(a,y)=0 \tag{25}$$
$$P_1(x,0,z)=0 \tag{26}$$
$$P_1(x,b,z)=0 \tag{27}$$
$$P_1(0,y,z)=0 \tag{28}$$
$$P_1(a,y,z)=0 \tag{29}$$
$$P_2(x,0,z)=0 \tag{30}$$
$$P_2(x,b,z)=0 \tag{31}$$
$$P_2(0,y,z)=0 \tag{32}$$
$$P_2(a,y,z)=0 \tag{33}$$

Since the normal velocity components and the pressures must be continuous at the interfaces

$$\left.\frac{\partial P_2}{\partial z}\right|_{z=h+H_1+H_2}=0 \tag{34}$$

$$k_1\left(\frac{\partial P_1}{\partial z}\right)_{z=h+H_1}=k_2\left(\frac{\partial P_2}{\partial z}\right)_{z=h+H_1} \tag{35}$$

$$P_1(x,y,h+H_1)=P_2(x,y,h+H_1) \tag{36}$$

$$p(x,y)=P_1(x,y,h) \tag{37}$$

The problem appears to be a coupled one according to equation (17) and using the coupled boundary conditions (35)-(37).

Solutions of equations (18) and (19) with the corresponding uncoupled boundary conditions are obtained as

$$P_1(x,y,z)=\sum_{m=1}^{\infty}\sum_{n=1}^{\infty}A_{mn}^1 Sin(\alpha_m x)Sin(\beta_n y)e^{\gamma_{mn}z/C_1}\left\{1+B_{mn}^1 e^{-2\gamma_{mn}z/C_1}\right\} \tag{38}$$

$$P_2(x,y,z)=\sum_{m=1}^{\infty}\sum_{n=1}^{\infty}A_{mn} Sin(\alpha_m x)Sin(\beta_n y)e^{\gamma_{mn}z/C_2}\left\{1+e^{-2\gamma_{mn}(z-h-H_1-H_2)/C_2}\right\} \tag{39}$$

where

$$\alpha_m=\frac{m\pi}{a},\quad \beta_n=\frac{n\pi}{b},\quad \gamma_{mn}^2=\alpha_m^2+\beta_n^2 \tag{40}$$

According to equation (37)

$$p(x,y)=\sum_{m=1}^{\infty}\sum_{n=1}^{\infty}B_{mn} Sin(\alpha_m x)Sin(\beta_n y) \tag{41}$$

With

$$B_{mn} = A^1_{mn} e^{\gamma_{mn} h/C_1} \left\{1 + B^1_{mn} e^{-2\gamma_{mn} h/C_1}\right\} \tag{42}$$

The solution of p as given by equation (41) satisfies conditions (22)-(25). From condition (36) we get

$$A^1_{mn} = \frac{A_{mn} e^{\gamma_{mn}(h+H_1)\left(\frac{1}{C_2}-\frac{1}{C_1}\right)} \left\{1 + e^{2\gamma_{mn} H_2/C_2}\right\}}{\left\{1 + B^1_{mn} e^{-2\gamma_{mn}(h+H_1)/C_1}\right\}} \tag{43}$$

Substituting equation (43) in equations (38) and (42) respectively gives

$$P_1(x,y,z) = \sum_{m=1}^{\infty}\sum_{n=1}^{\infty} A_{mn} G_{mn} e^{\gamma_{mn}(z-h)/C_1} \frac{\left\{1 + B^1_{mn} e^{-2\gamma_{mn} z/C_1}\right\}}{\left\{1 + B^1_{mn} e^{-2\gamma_{mn}(h+H_1)/C_1}\right\}} Sin\left(\alpha_m x\right) Sin\left(\beta_n y\right) \tag{44}$$

and

$$B_{mn} = A_{mn} G_{mn} \left\{\frac{1 + B^1_{mn} e^{-2\gamma_{mn} h/C_1}}{1 + B^1_{mn} e^{-2\gamma_{mn}(h+H_1)/C_1}}\right\} \tag{45}$$

where

$$G_{mn} = e^{\gamma_{mn}(h+H_1)\left(\frac{1}{C_2}-\frac{1}{C_1}\right)} \left\{1 + e^{2\gamma_{mn} H_2/C_2}\right\} e^{\gamma_{mn} h/C_1} \tag{46}$$

From equation (35) we get

$$B^1_{mn} = \left(\frac{1 - F_{mn}}{1 + F_{mn}}\right) e^{2\gamma_{mn}(h+H_1)/C_1} \tag{47}$$

where

$$F_{mn} = \left(\frac{k_2 C_1}{k_1 C_2}\right) \frac{\left(1 - e^{2\gamma_{mn} H_2/C_2}\right)}{\left(1 + e^{2\gamma_{mn} H_2/C_2}\right)} \tag{48}$$

Substitution of equations (45) and (47) in equation (41) yields

$$p(x,y) = \frac{1}{2}\sum_{m=1}^{\infty}\sum_{n=1}^{\infty} A_{mn} G_{mn} \left\{1 + F_{mn} + \left(1 - F_{mn}\right) e^{2\gamma_{mn} H_1/C_1}\right\} Sin\left(\alpha_m x\right) Sin\left(\beta_n y\right) \tag{49}$$

Substituting equation (47) in equation (44) gives

$$P_1(x,y,z) = \frac{1}{2}\sum_{m=1}^{\infty}\sum_{n=1}^{\infty} A_{mn} G_{mn} e^{\gamma_{mn}(z-h)/C_1} \left\{1 + F_{mn} + \left(1 - F_{mn}\right) e^{2\gamma_{mn}(h+H_1-z)/C_1}\right\} Sin\left(\alpha_m x\right) Sin\left(\beta_n y\right) \tag{50}$$

Using equations (49) and (50) in equation (17) and simplifying gives

$$\frac{dh}{dt} = \frac{1}{2}\sum_{m=1}^{\infty}\sum_{n=1}^{\infty} A_{mn} G_{mn} C_{mn} \left\{1 + F_{mn} + \left(1 - F_{mn}\right) e^{2\gamma_{mn} H_1/C_1}\right\} Sin\left(\alpha_m x\right) Sin\left(\beta_n y\right) \tag{51}$$

where

$$C_{mn} = \left(\frac{k_1 \gamma_{mn}}{\mu C_1}\right) \frac{\left\{1 + F_{mn} - \left(1 - F_{mn}\right) e^{2\gamma_{mn} H_1/C_1}\right\}}{\left\{1 + F_{mn} + \left(1 - F_{mn}\right) e^{2\gamma_{mn} H_1/C_1}\right\}} - \frac{\gamma^2_{mn} h_0^2}{\mu M_0^2} f(h,l,M_0) \tag{52}$$

The constants A_{mn} are determined using orthogonality of Eigen functions $Sin\alpha_{mn} x$ and $Sin\beta_{mn} x$ in equation (51) as

$$\frac{dh}{dt} = \frac{1}{2}\sum_{m=1}^{\infty} \frac{a}{2}\frac{b}{2}$$

$$A_{mn} = \begin{cases} \dfrac{32(dh/dt)}{\pi^2 mn} \times \dfrac{1}{G_{mn} C_{mn} \left\{1 + F_{mn} + \left(1 - F_{mn}\right) e^{2\gamma_{mn} H_1/C_1}\right\}} & m,n \ are \ odd \\ 0 & otherwise \end{cases} \tag{53}$$

Substituting equation (53) in equation (49) the pressure distribution in the film region is obtained as

$$p(x,y) = \sum_{m=1,3,5...}^{\infty}\ \sum_{n=1,3,5...}^{\infty} \frac{16(dh/dt)}{\pi^2 mn C_{mn}} Sin\left(\alpha_m x\right) Sin\left(\beta_n y\right) \tag{54}$$

In non dimensional form it becomes

$$p^*(x,y) = -\frac{ph^3}{(dh/dt)\mu a^2} = \frac{16}{\pi^3}\sum_{m=1,3,5...}^{\infty}\sum_{n=1,3,5...}^{\infty}\frac{Sin(\alpha_m x)Sin(\beta_n y)}{mn(m^2+d^2n^2)^{1/2}\left[\frac{\pi(m^2+d^2n^2)^{1/2}}{M_0^2h^{*3}}G(h^*,l^*,M_0)+\frac{\psi_1}{C_1h^{*3}}D_{mn}\right]} \tag{55}$$

Where

$$h^* = \frac{h}{h_0}, H^* = \frac{H}{a}, \psi_1 = \frac{k_1H}{h_0^3} \tag{56}$$

$$D_{mn} = \frac{1}{H^*}\frac{\left\{(1-F_{mn})e^{2\gamma_{mn}H_1/C_1}-(1+F_{mn})\right\}}{\left\{(1-F_{mn})e^{2\gamma_{mn}H_1/C_1}+(1+F_{mn})\right\}} \tag{57}$$

The load carrying capacity is determined by integrating the pressure over the area of the plate:

$$w = \int_0^a\int_0^b p^*(x,y)dxdy \tag{58}$$

In dimensionless form it is obtained as

$$W^* = -\frac{wh^3}{(dh/dt)\mu a^3 b}$$

$$= \frac{64}{\pi^5}\sum_{m=1,3,5...}^{\infty}\sum_{n=1,3,5...}^{\infty}\frac{1}{m^2n^2(m^2+d^2n^2)^{1/2}\left[\frac{\pi(m^2+d^2n^2)^{1/2}}{M_0^2h^{*3}}G(h^*,l^*,M_0)+\frac{\psi_1}{C_1h^{*3}}D_{mn}\right]} \tag{59}$$

From equation (59), the time of the approach as a function of the height h given by

$$\Delta t = -\frac{\mu a^3 b}{wh_0^2}\frac{64}{\pi^5}\sum_{m=1,3,5...}^{\infty}\sum_{n=1,3,5...}^{\infty}\frac{M_0^2}{\pi m^2n^2(m^2+d^2n^2)}\int_1^{h^*}\frac{1}{\left[G(h^*,l^*,M_0)+E_{mn}\right]}dh^* \tag{60}$$

where

$$E_{mn} = \frac{\psi_1 M_0^2 D_{mn}}{C_1\pi(m^2+d^2n^2)^{1/2}} \tag{61}$$

Assuming that the initial film thickness is h_0 at $t_0 = 0$, the time of approach in dimensionless form is obtained as

$$\Delta T = \frac{wh_0^2}{\mu a^3 b}\Delta t = -\frac{64}{\pi^6}\sum_{m=1,3,5...}^{\infty}\sum_{n=1,3,5...}^{\infty}\frac{M_0^2}{m^2n^2(m^2+d^2n^2)}\int_1^{h^*}\frac{1}{\left[E_{mn}+G(h^*,l^*,M_0)\right]}dh^* \tag{62}$$

In particular when $l^* \to 0$ equation (59) and (61) reduces to the results obtained by M.V Bhat and J.V Hingu[5].

4. RESULTS AND DISCUSSION

In the present paper, the Modified Reynolds Equation is obtained for the squeeze film characteristics of double layered porous rectangular plates in the presence of magnetic field and conducting couple stresses with respect to the various dimensionless parameters k_2/k_1, M_0 and l^* .The parameter k_2/k_1 is permeability parameter and M_0 is the Hartmann number, which signifies an enhancement in the squeeze film pressure. l^* arises due to the presence of polar additives in the lubricant and the length of l may be regarded as the chain length of the polar additives in the lubricant. The parameter l^* yields the mechanism of interaction of the fluid with bearing geometry. The additives effects are more prominent when either the chain length of polar additives is large or the minimum film thickness is small. Hence, the squeeze film characteristics of double layered porous rectangular plates are analyzed for the combined effect of conducting couple stress parameter and magnetic parameter.

4.1 PRESSURE DISTRIBUTION

Figure 2 depicts the variation of non-dimensional pressure p^* with x^* for different values of M_0 for both Newtonian (l^* =0) and CCSF (l^* =0.4) with $H^* = 0.4, \lambda = 1, y^* = 0.5$. It is observed that p^* increases for increasing the values of

M_0 for both values of l^*. The variation of non-dimensional pressure p^* with x^* for different values of k_2/k_1 is shown in Figure 3. It is observed that the increasing values of k_2/k_1 shows decrease in p^*. The variation of non-dimensional pressure p^* with x^* for different values of ψ is shown in Figure 4. It is observed that the increasing values of ψ shows the significant decrease in p^*.

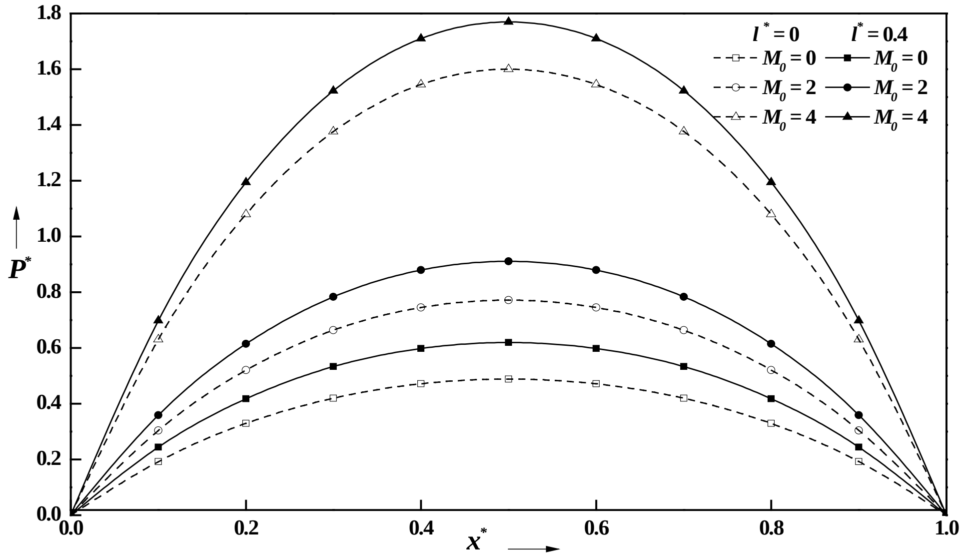

Figure-2. Variation of non-dimensional Pressure p^* with x^* for different values of l^* and M_0 with $\overset{*}{h} = 1.2$, $\overset{*}{y} = 0.5$, $\psi = 0.001$, $a = 1$, $b = 1$, $\beta = 0.2$, $H_1 = 0.001$, $H_2 = 0.002$, $m_1 = m_2 = 0.6$, $k_1 = 0.01$, $k_2 = 0.1$

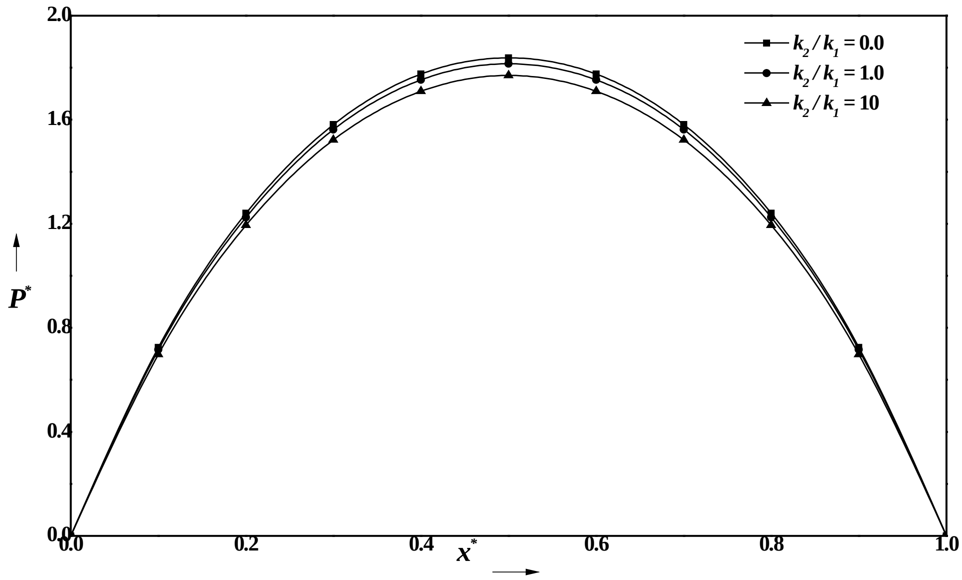

Figure-3. Variation of non-dimensional Pressure p^* with x^* for different values of k_2/k_1 with $M_0 = 4$, $l^* = 0.4$, $\overset{*}{h} = 1.2$, $\overset{*}{y} = 0.5$, $\psi = 0.001$, $a = 1$, $b = 1$, $\beta = 0.2$, $H_1 = 0.001$, $H_2 = 0.002$, $m_1 = m_2 = 0.6$.

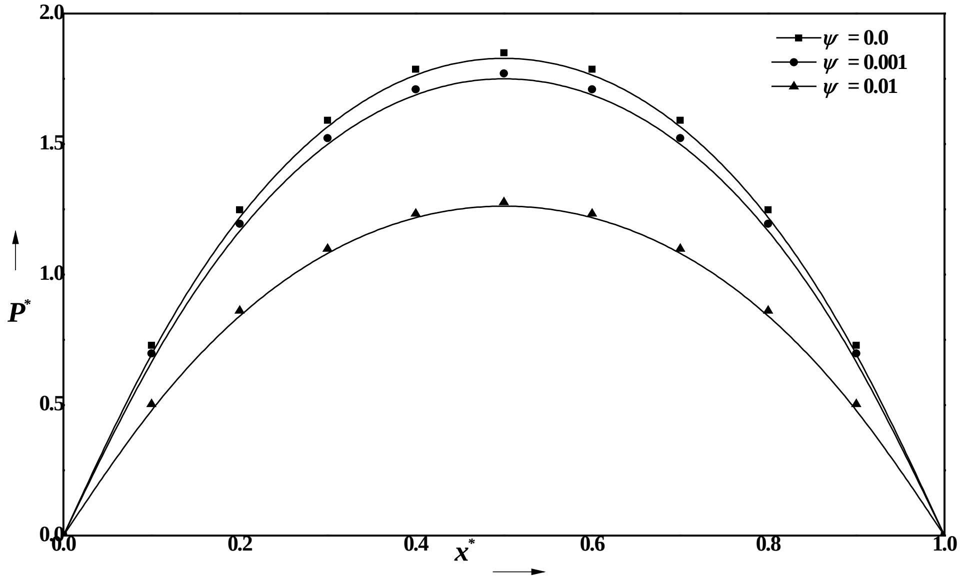

Figure-4. Variation of non-dimensional Pressure p^* with x^* for different values of ψ with $M_0 = 4$, $l^* = 0.4$, $\overset{*}{h} = 1.2$, $\overset{*}{y} = 0.5$, $a = 1$, $b = 1$, $\beta = 0.2$, $H_1 = 0.001$, $H_2 = 0.002$, $m_1 = m_2 = 0.6$ $k_1 = 0.01$, $k_2 = 0.1$.

4.2 LOAD CARRYING CAPACITY

The variation of non-dimensional load carrying capacity W^* with h^* for different values of M_0 for two values of l^* is shown in Figure 5. Here the dotted lines represent the Newtonian case and solid lines represent the couplestress case. It is observed that W^* increases for increasing values of M_0 as compared to the corresponding non-magnetic case. From the figure it is also clear that, the effect of couplestress is to increase W^* as compared to the Newtonian case. The variation of non-dimensional load carrying capacity W^* with h^* for different values of k_2/k_1 is shown in Figure 6. It is observed that the increasing values of k_2/k_1 shows decrease in W^*. The variation of non-dimensional load carrying capacity W^* with h^* for different values of ψ is shown in Figure 7. It is observed that the increasing values of ψ shows decrease in W^*.

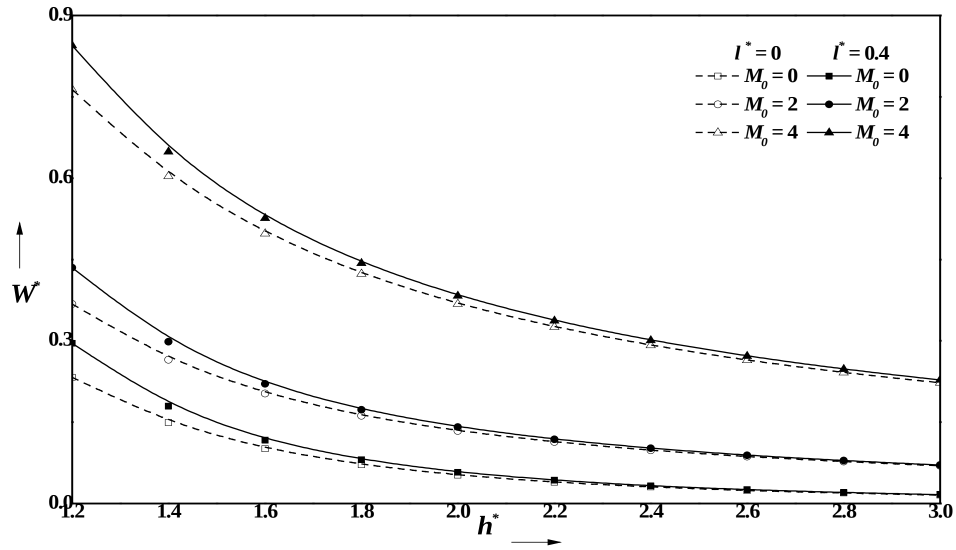

Figure-5. Variation of non-dimensional Load carrying capacity W^* with $\overset{*}{h}$ for different values of l^* and M_0 with $\psi = 0.001$, $a = 2$, $b = 1$, $\beta = 0.2$, $H_1 = 0.001$, $H_2 = 0.002$, $m_1 = m_2 = 0.6$, $k_1 = 0.01$, $k_2 = 0.1$

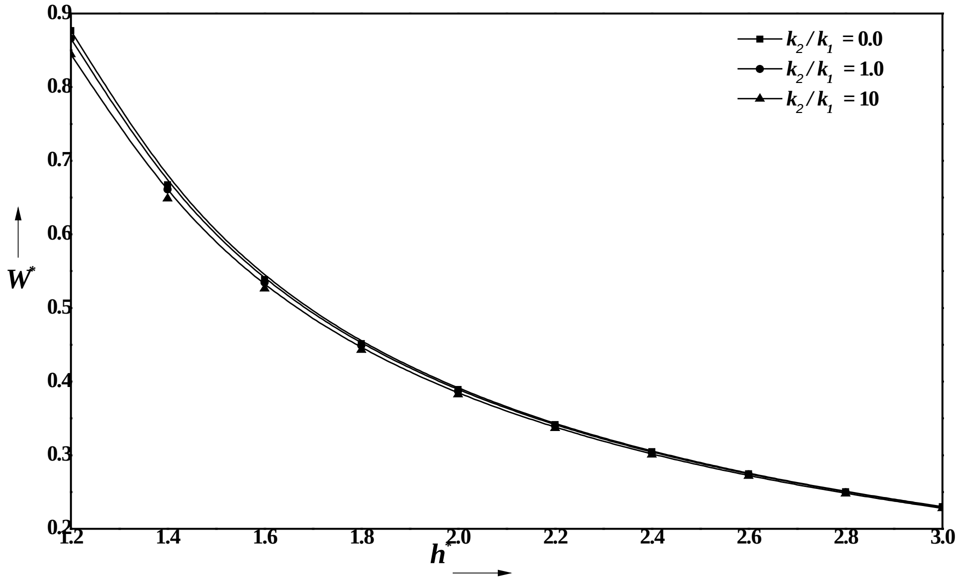

Figure-6. Variation of non-dimensional Load carrying capacity W^* with h^* for different values of k_2/k_1 with $M_0 = 4$, $l^* = 0.4$, $\psi = 0.001$, $a = 2$, $b = 1$, $\beta = 0.2$, $m_1 = m_2 = 0.6$, $H_1 = 0.001$, $H_2 = 0.002$.

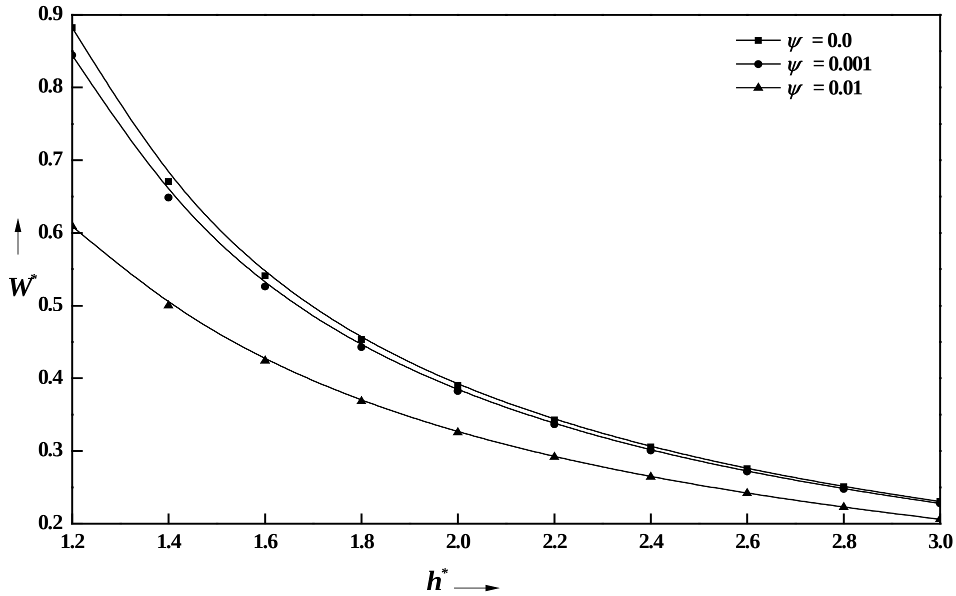

Figure-7. Variation of non-dimensional Load carrying capacity W^* with h^* for different values of ψ with $M_0 = 4$, $l^* = 0.4$, $a = 2$, $b = 1$, $\beta = 0.2$, $H_1 = 0.001$, $H_2 = 0.002$, $m_1 = m_2 = 0.6$, $k_1 = 0.01$, $k_2 = 0.1$

4.3 SQUEEZE FILM TIME

The variation of nondimensional squeeze film time T^* with h^* for different values of M_0 for two values of l^* is shown in Figure 8. Here the solid lines corresponds to the couplestress case $(l^* = 0.4)$ and the dashed lines corresponds to the Newtonian case $(l^* = 0)$. It is observed that T^* increases as M_0 increases, it is also observed that effect of couplestress is to increase T^* as compared to Newtonian case. The variation of nondimensional squeeze film time T^* with h^* for different values of k_2/k_1 is shown in Figure 9. It is observed that T^* decreases as k_2/k_1 increases. The variation of non dimensional squeeze film time T^* with h^* for different values of ψ is shown in Figure 10. It is observed that T^* decreases as ψ increases.

The effect of transverse magnetic field on the squeeze film characteristics is evaluated by the relative percentage difference. The increase in the non-dimensional load carrying capacity R_{W^*} and non-dimensional squeeze film time R_{T^*} are defined by

$$R_{W^*} = \left\{ \left(W^*_{magnetic} - W^*_{non-magnetic} \right) / W^*_{non-magnetic} \right\} \times 100 ,$$

$$R_{T^*} = \left\{ \left(T^*_{magnetic} - T^*_{non-magnetic} \right) / T^*_{non-magentic} \right\} \times 100 .$$

The values of R_{w^*} and R_{T^*} is listed in Table 1 for various values of l^* and M_0. It is observed that, an increase of 54.96 % and 32.40 % is observed in R_{w^*} and R_{T^*} respectively for $M_0 = 2$ and $l^* = 0.2$. Table 2 and 3 shows the variation l^* and M_0 for increasing values of k_2/k_1. It is observed that increasing values of k_2/k_1 is to decrease W^* and T^*.Also as $l^* \to 0$ the results are in close agreement with results obtained by M.V Bhat and J.V Hingu[5].

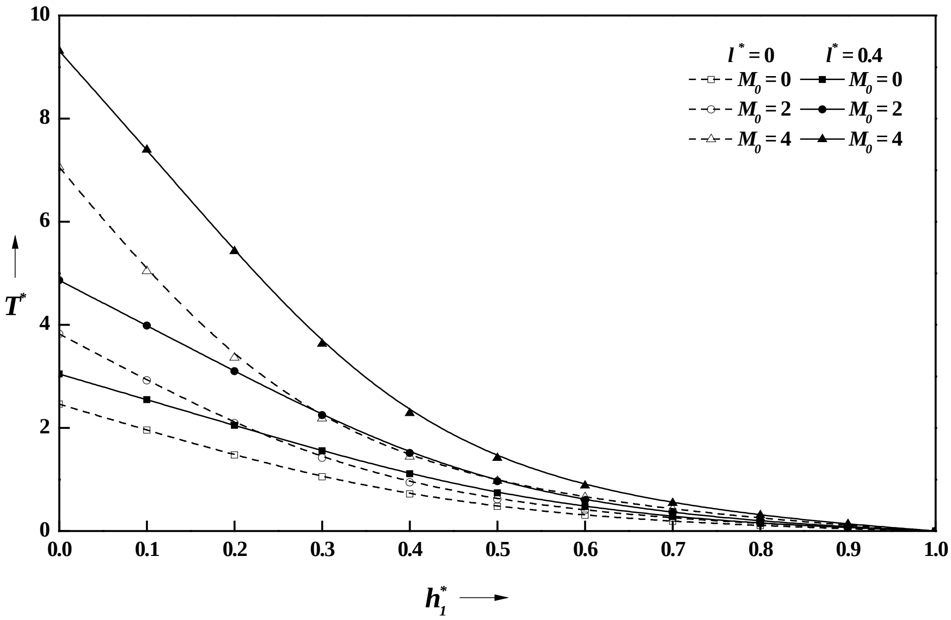

Figure-8. Variation of non-dimensional Squeeze film time T^* with h^* for different values of l^* and M_0 with $\psi = 0.001$, $a = 2$, $b = 1$, $\beta = 0.2$, $H_1 = 0.001$, $H_2 = 0.002$, $m_1 = m_2 = 0.6$, $k_1 = 0.01$, $k_2 = 0.1$

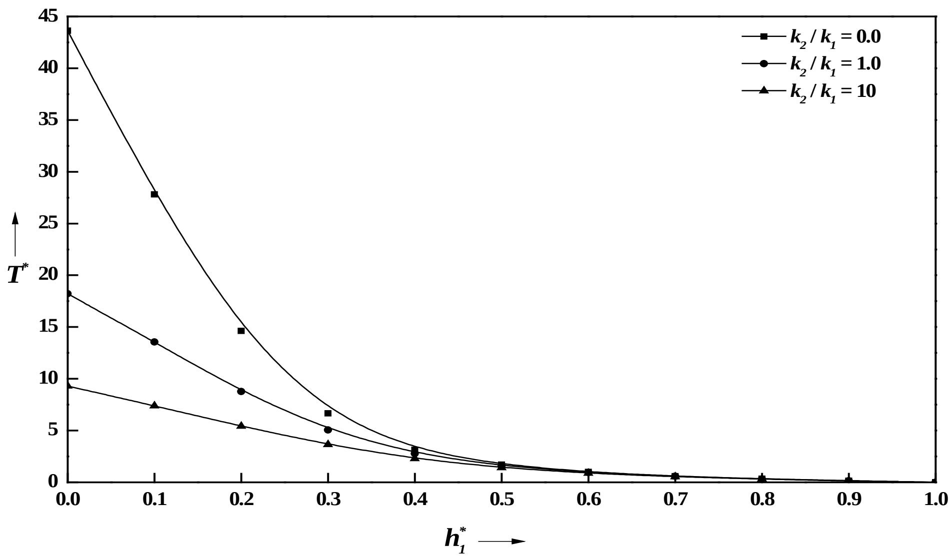

Figure-9. Variation of non-dimensional Squeeze film time T^* with h^* for different values of k_2/k_1 with $M_0 = 4$, $l^* = 0.4$, $\psi = 0.001$, $a = 2$, $b = 1$, $\beta = 0.2$, $H_1 = 0.001$, $H_2 = 0.002$, $m_1 = m_2 = 0.6$.

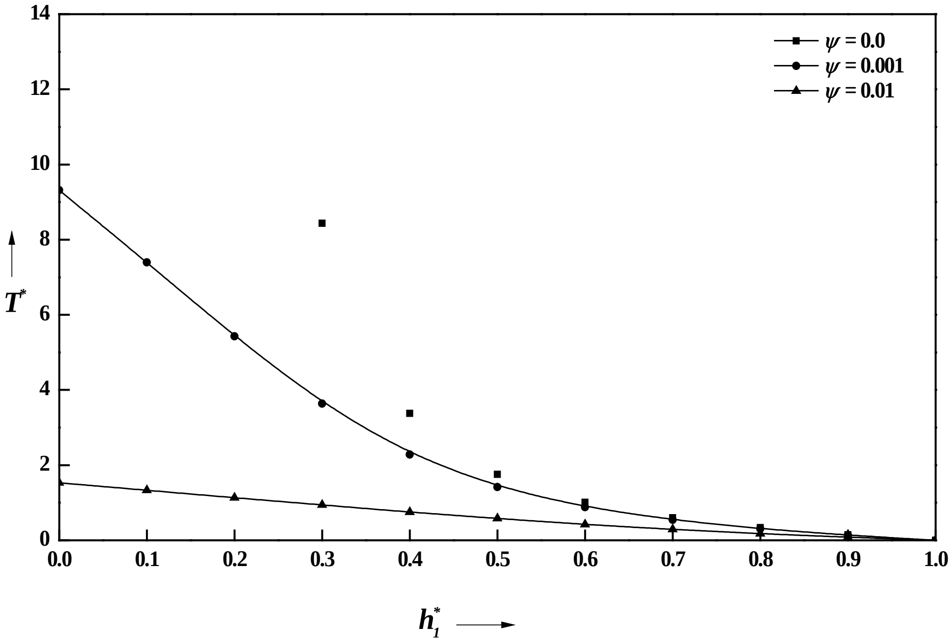

Figure-10. Variation of non-dimensional Squeeze film time T^* with h^* for different values of ψ with $M_0 = 4$, $l^* = 0.4$, $a = 2$, $b = 1$, $\beta = 0.2$, $m_1 = m_2 = 0.6$, $H_1 = 0.001$, $H_2 = 0.002$, $k_1 = 0.01$, $k_2 = 0.1$.

Table .1: Variation of R_{W^*} and R_{T^*} with l^* for different values M_0 with $h^* = 1.2$, $a = 1$, $b = 1$, $\psi = 0.001$, $H_1 = 0.001$, $H_2 = 0.002$, $m_1 = m_2 = 0.6$, $\beta = 0.2$, $k_1 = 0.01$, $k_2 = 0.1$.

l^*	M_0	R_{W^*}	R_{T^*}
0	1	14.62461	8.765499
	2	58.07563	30.99211
	3	129.501	61.93706
0.1	1	14.41786	8.914313
	2	57.30701	31.36239
	3	127.9022	62.19261
0.2	1	13.82228	9.310899
	2	54.96696	32.40653
	3	122.8094	63.13458
0.3	1	12.91926	9.884685
	2	51.36157	34.17019
	3	114.8072	65.55628

Table-2: The variation of non –dimensional load carrying capacity W^* with different values of Hartmann number M_0, couplestress parameter l^* and k_2/k_1 with $\psi = 0.001, \beta = 0.2, h_2^* = 0.5$.

Hartmann Number	Permeability ratio	M.V.Bhat et al for W^*	Present analysis for W^*		
		$l^* = 0$	$l^* = 0$	$l^* = 0.1$	$l^* = 0.2$
$M_0 = 0$	$k_2/k_1 = 0$	0.625954	0.625910	0.686047	0.851775
	$k_2/k_1 = 1.0$	0.532650	0.532618	0.575549	0.687823
	$k_2/k_1 = 10$	0.227525	0.227519	0.235007	0.251789
$M_0 = 1$	$k_2/k_1 = 0$	0.643801	0.641376	0.701611	0.867461

	$k_2/k_1=1.0$	0.550773	0.545470	0.588434	0.700809
	$k_2/k_1=10$	0.309400	0.258096	0.267332	0.288337
$M_0=2$	$k_2/k_1=0$	0.696508	0.687562	0.748273	0.914500
	$k_2/k_1=1.0$	0.603622	0.583862	0.627066	0.739747
	$k_2/k_1=10$	0.454770	0.335501	0.349331	0.381723

Table-3: The variation of non –dimensional squeezing time T^* for different values of Hartmann number M_0, couplestress parameter l^* and k_2/k_1 with $\psi=0.001, \beta=0.2, h_2^*=0.5$.

Hartmann Number	Permeability ratio	M.V.Bhat et al for T^*	Present analysis for T^*		
		$l^*=0$	$l^*=0$	$l^*=0.1$	$l^*=0.2$
$M_0=0$	$k_2/k_1=0$	2.50381	2.50564	2.74419	3.4071
	$k_2/k_1=1.0$	2.13060	2.13192	2.30220	2.75129
	$k_2/k_1=10$	0.910099	0.91034	0.940028	1.00715
$M_0=1$	$k_2/k_1=0$	2.57520	2.56456	2.80644	3.46984
	$k_2/k_1=1.0$	2.20309	2.17986	2.35374	2.80324
	$k_2/k_1=10$	1.23760	1.01076	1.06933	1.15335
$M_0=2$	$k_2/k_1=0$	2.78603	2.74643	2.99309	3.65800
	$k_2/k_1=1.0$	2.41449	2.32724	2.50826	2.95899
	$k_2/k_1=10$	1.81908	1.27610	1.39732	1.52689

5. CONCLUSION

On the basis of MHD and stokes theory for couplestress, the Modified Reynolds Equation for the squeeze film characteristics of double-layered porous rectangular plates with CCSF and transverse magnetic field is obtained. According to the above results and discussions, conclusion can be drawn as follows.

- The combined effect of M_0 and l^* is to increase the non-dimensional squeeze pressure p^*, load carrying capacity $\overset{*}{W}$ and squeeze film time T^*.
- For NCL case $(l^* \to 0)$ these results reduces to M.V Bhat and J.V Hingu [5] case.
- Further results in Table 1-3 are provided for engineering applications. From the Tables it is observed that there is significant increase in non-dimensional pressure, load carrying capacity and squeeze film time for increasing values of couplestresses l^*.
- Further it is interesting to note that increasing values of k_2/k_1 is to decrease the squeeze film characteristics.

NOMENCLATURE

B_0	Applied magnetic field
a b	Length and width of plate
A_{mn} A'_{mn} B_{mn} B'_{mn}	Defined in Eqs. (53), (43), (42) and (47)
C_{mn} D_{mn} E_{mn} F_{mn} G_{mn}	Defined in Eqs. (52), (57), (61) (48) and (46)
c_1 c_2	Defined in Eqs. (20) and (21)
h	Film thickness
h_0	Initial film thickness
h^*	Non-dimensional film thickness (h/h_0)
H	H_1+H_2
H_1, H_2	Thicknesses of the lower and upper porous layers
H^*	H/a
k_1, k_2	Permeability of the lower and upper porous layers
m_1, m_2	Porosities of the lower and upper porous layers
M_0	Hartmann number $\left(= B_0 h_0 (\sigma/\mu)^{1/2}\right)$

p	Pressure in the film region
p^*	Non-dimensional pressure $\left(-\frac{dt}{dh}\frac{h^3 p}{\mu a^2}\right)$
P_1, P_2	Pressures in the lower and upper porous layers
t_0	Time of initial film thickness
t_1	Time of the film thickness h_1
Δt	Time required for the film thickness h_1
ΔT	Non-dimensional time Δt
u, v, w	Velocity components in the film region
u_1, v_1, w_1	Velocity components in the lower porous layer
u_2, v_2, w_2	Velocity components in the upper porous layer
W	Load capacity
W^*	Non-dimensional load capacity $\left(-\frac{dt}{dh}\frac{h^3 W}{\mu a^3 b}\right)$
x, y, z	Rectangular coordinates
$\alpha_m, \beta_n, \gamma_{mn}, d$	Defined in eqn. (40)
μ	Absolute viscosity
ξ_1, ξ_2	Dummy variables
σ	Conductivity of the fluid
ψ_1	Defined in eqn. (56)

REFERENCES

1. Morgan V.T. and Cameron A., Mechanism of lubrication in porous metal bearings. Lubrication and Wear Institution of Mechanical Engineers .89, (1957), pp.151-157.
2 Wu H., Analysis of the squeeze film between porous rectangular plates. Journal of Lubrication Technology, Transaction ASME. 94, (1972), pp.64-68.
3 Uma S., The analysis of double layered porous slider bearings. Wear .42. (1977), pp.205-215.
4 Prakash J, and Vij S.K., Load capacity and time height relations for squeeze films between porous plates.Wear 24. (1973)309-322.
5 Bhat M.V.and Hingu J.V., A study of the hydromagnetic squeeze film between two- layered porous rectangular plates. Wear .50, (1978), pp.1-10.
6 Cusano C.,Lubrication of a two layered porous journal bearing. Journal of Mechanical Engineering Science.14, (1972), pp.335-339.
7 Stokes V.K., Couple stresses in fluids. Physics of fluids .9,(1966),pp.1709-1715.
8 Naduvinamani N.B, Hiremath P.S,and Gurubasawaraj G., Squeeze film lubrication of a short porous journal bearing with a couplestress fluid. Tribology International .34.(2001), pp.739-747.
9 Ramanaiha G., Squeeze films between finite plates lubricated by fluids with couple stresses. Wear. 54.(1979), pp.315-320.
10 Bujurke N.M. and Jayaraman G., The influence of couple stresses in squeeze Films. International journal of Mechanical science.24,(1982),pp.369-376.
11 Maki E.R, and Kuzma D.C., Magneto-hydrodynamic Lubrication Flow Between Parallel Plates. Jounal of fluid Mechanics.26,(1966), pp.534-543.
12 Kumiyama S., Magneto-hydrodynamics journal bearing (report I). Journal of lubrication Technology.91,(1969), pp.380-386.
13 Jaw-Ren Lin., MHD squeeze film characteristics for finite rectangular plates. Industrial Lubrication and Tribology.55,(2003),pp.84-89.
14 Lin JR. Magneto-hydrodynamic squeeze film characteristics for finite rectangular plates. Industrial lubrication and tribology.55 (2), (2003), pp.84-89.
15 Sinha P.C, and Gupta J.L,. Hydromagnetic squeeze film between porous rectangular Plates. Journal of lubrication Technology ASME series F195, (1973), pp. 394-398.

16 Naduvinamani N.B, Fathima S.T, and Hanumagouda B.N., Magneto-hydrodynamic couple stress squeeze film lubrication of circular stepped plates. Proceedings Mechnical engineering Part I, journal of Engineering Tribology.225, (2010),pp.1-9.

Source of support: Nil, Conflict of interest: None Declared